Future Atmospheric Rivers and Impacts on Precipitation: Overview of the ARTMIP Tier2 High-Resolution Global Warming Experiment

Christine A. Shields[1*], Ashley E. Payne[2,3*], Eric J. Shearer[4,], Michael F. Wehner[5], Travis A. O'Brien[6,7], Jonathan J. Rutz[8], L. Ruby Leung[9], F. Martin Ralph[10], Allison B. Marquardt Collow[11,12], Paul A. Ullrich[13], Qizhen Dong[14], Alexander Gershunov[10,], Helen Griffith[15], Bin Guan[16], Juan M. Lora[17], Mengqian Lu[14], Elizabeth McClenny[13], Kyle M. Nardi[18], Mengxin Pan[14], Yun Qian[9], Alexandre M. Ramos[19,20], Tamara Shulgina[10], Maximiliano Viale[21] Chandan Sarangi[9, 22], Ricardo Tomé[20], Colin Zarzycki[18]

*These authors contributed equally to this work

[1]Climate and Global Dynamics Division, National Center for Atmospheric Research, Boulder, CO, 80302, USA

[2]Department of Climate and Space Sciences and Engineering, University of Michigan, Ann Arbor, MI, 48109, USA

[3]Tomorrow.io, Boston, MA 02210, USA

[4]Center for Hydrometeorology and Remote Sensing, University of California, Irvine, Irvine, CA, USA

[5]Applied Mathematics and Computational Research Division, Lawrence Berkeley National Laboratory, Berkeley, CA, USA

[6]Dept. of Earth and Atmospheric Sciences, Indiana University, Bloomington, IN, USA

[7]Climate and Ecosystem Sciences Division, Lawrence Berkeley National Laboratory, Berkeley, CA, USA

[8]National Weather Service, Western Region Headquarters, Science and Technology Infusion Division, Salt Lake City, UT, USA

[9]Pacific Northwest National Laboratory, Richland, WA, USA

[10]Center for Western Weather and Water Extremes, Scripps Institution of Oceanography, University of California, San Diego, La Jolla, CA, USA

[11]University of Maryland Baltimore County, Baltimore, MD, USA

[12]Global Modeling and Assimilation Office, NASA Goddard Space Flight Center, Greenbelt, MD, USA
[13]Dept. of Land, Air and Water Resources, University of California, Davis, Davis, CA, USA
[14] Department of Civil and Environmental Engineering, The Hong Kong University of Science and Technology, Clear Water Bay, Kowloon, Hong Kong
[15] Department of Geography and Environmental Science, University of Reading, Reading, UK
[16]Joint Institute for Regional Earth System Science and Engineering, University of California, Los Angeles, CA, USA
[17]Dept. of Earth and Planetary Sciences, Yale University, New Haven, CT, USA
[18]Dept. of Meteorology and Atmospheric Science, Pennsylvania State University, University Park, PA, USA
[19] Institute of Meteorology and Climate Research, Karlsruhe Institute of Technology, Karlsruhe, Germany
[20]Universidade de Lisboa, Faculdade de Ciências, Instituto Dom Luiz, Lisboa, Portugal
[21] Instituto Argentino de Nivología, Glaciología y Ciencias Ambientales (IANIGLA-CONICET), Mendonza, Argentina
[22] Department of Civil Engineering, Indian Institute of Technology Madras, Chennai, India

Key Points:

- High-resolution historical and future simulations are used to evaluate Atmospheric River Detection Tools (ARDT) uncertainty
- ARDTs mostly show increases in frequency and intensity of future ARs but the scale of response is dependent on algorithmic restrictiveness
- Most regions experience an increase in precipitation volume coming from extreme ARs

Corresponding author: Christine A. Shields (shields@ucar.edu) manuscript submitting to GRL

Abstract

Atmospheric rivers (ARs) are long, narrow synoptic scale weather features important for Earth's hydrological cycle typically transporting water vapor poleward, delivering precipitation important for local climates. Understanding ARs in a warming climate is problematic because the AR response to climate change is tied to how the feature is defined. The Atmospheric River Tracking Method Intercomparison Project (ARTMIP) provides insights into this problem by comparing 16 atmospheric river detection tools (ARDTs) to a common dataset consisting of high resolution climate change simulations from a global atmospheric general circulation model. ARDTs mostly show increases in frequency and intensity, but the scale of the response is largely dependent on algorithmic criteria. Across ARDTs, bulk characteristics suggest intensity and spatial footprint are inversely correlated, and most focus regions experience increases in precipitation volume coming from extreme ARs. The spread of the AR precipitation response under climate change is large and dependent on ARDT selection.

Plain Language Summary

Atmospheric rivers (ARs) are long and narrow weather features often referred to as "rivers in the sky". They often transport water from lower latitudes to higher latitudes typically across climate zones and produce precipitation necessary for local climates. Understanding ARs in a warming climate is challenging because of the variety of ways an atmospheric river can be defined on gridded datasets. Unlike weather features such as tropical cyclones where identification methodologies are similar, algorithms that determine the characteristics of ARs vary depending on the science question posed. Because there is no real consensus on AR identification methodology, we aim to quantify the algorithmic uncertainty in AR metrics and precipitation. We compare 16 different ways of defining an AR on gridded datasets and present the range of possibilities in which an AR could change under global warming. Generally, ARs are projected to increase but the amount of that increase is a function of the algorithm. Across all algorithms and focus regions, AR precipitation is projected to become more extreme.

1 Introduction

The intersection of climate change and atmospheric rivers (ARs) can be characterized as a cross-disciplinary study that spans physical and social sciences across the globe (e.g., Reid et al., 2022; Sadeghi et al., 2021; Albano et al., 2020; Payne et al., 2020; Corringham et al., 2022; Viale et al., 2018; Espinoza et al., 2018; Ralph et al., 2017; Ramos et al., 2015; Blamey et al., 2015; Lavers et al. 2013; Baek and Lora, 2021). ARs are synoptic scale weather features, longer than wide, that serve as water and energy transport vehicles (Zhu and Newell 1998). They are usually attached to a baroclinic zone or extratropical cyclones, typically travel meridionally across latitudes or climate zones and are an important component of Earth's hydrological cycle (Ralph et al., 2018, AMS Glossary of Meteorology). ARs are highly relevant to any populated region around the globe that depends on precipitation for a source of water and thus changes to these weather features are important for managing evolving water resources (e.g., Rhoades et al., 2021; Pan and Lu, 2020; Griffiths et al., 2020; Schick et al., 2020, Sousa et al., 2018; Paltan et al., 2017). Despite the attention to ARs and climate change in the literature, much remains uncertain. AR characteristics, such as size, shape, and intensity, are tightly bound to how we define them and firmly tied to the science question being asked (Ralph et al., 2018; Shields et al., 2019; O'Brien et al., 2020). Atmospheric river detection tools (ARDTs) that identify ARs in datasets reflect diverse perspectives of what constitutes an AR. Given ARDTs are developed for unique and often complementary scientific questions or purposes, they are also widely varied in their methodology. The Atmospheric River Tracking Method Intercomparison Project (ARTMIP) was designed to quantify the uncertainties in AR science that arise solely from detection/definition methodology (Rutz et al., 2019; Shields et al., 2018, Ralph et al., 2019; Lora et al., 2020). There have been numerous applications and publications utilizing ARTMIP data (summarized at https://www.cgd.ucar.edu/projects/artmip/publications.html), with the most recent publications featuring a reanalysis intercomparison and a climate change modelling intercomparison using CMIP5 and CMIP6 (Coupled Model Intercomparison Project Phases 5/6). The reanalysis intercomparison highlights precipitation attributable to ARs across ARDTs and reanalysis products (Collow et al., 2022), and the CMIP5/CMIP6 modelling intercomparison focuses on climate change trends (O'Brien et al., 2022). Both of these studies robustly show that uncertainty across ARDTs is larger than the uncertainty across climate models and reanalysis products.

For many ARDTs, the most impactful component determining whether an AR exists is the moisture threshold (Shields et al., 2018). Therefore, by definition, moisture thresholds directly impact the AR frequency such that methods with absolute threshold values, or relative threshold values computed using a fixed historical climatology, will produce higher AR frequency values compared to other methodologies when air temperatures are higher (e.g., global warming experiments where the Clausius-Clapeyron relationship dictates that the increase in air temperature translates into increased background moisture; O'Brien et al. 2022). Here, we build on this basic concept and explore projected changes in AR characteristics such as size, intensity, seasonality, and precipitation across regional and global ARDTs, using a high horizontal resolution global atmospheric general circulation model. Compared to lower resolution models, high resolution models better represent local geography and topography, as well as extreme precipitation and AR characteristics (Payne et al., 2020; Demory et al., 2020; Shields et al., 2016; Guan and Waliser, 2017). This paper is divided into four additional sections. Section 2 discusses data and approach and includes a discussion of the unique aspects of this high-resolution study; section 3 presents a global overview for context amongst previous ARTMIP studies; section 4 presents the regional view and ends with a discussion and summary in section 5.

2 Data and Approach

2.1 Model and Reanalysis

Precipitation, vertically Integrated Water Vapor (IWV) and Integrated Vapor Transport (IVT) were calculated from two integrations of a high horizontal resolution (~25km) version of the finite volume dynamical core version of the Community Atmosphere Model (fvCAM5.1). This global Atmospheric General Circulation Model (AGCM) was first forced by realistic sea surface temperatures and sea ice extent over the historical period of 1979-2005 (Wehner et al. 2014) under the protocols from the Atmospheric Model Intercomparison Project (AMIP) and will be referred to as "All-Hist". The AMIP surface boundary conditions were then perturbed to

represent a warmer world using output of the Community Earth System Model (CESM1), a fully coupled Ocean Atmospheric General Circulation Model (Hurrell et al., 2013). Monthly perturbations were defined as the difference between a CESM1 simulation forced under Representative Concentration Pathway (RCP) 8.5 (van Vuuren et al., 2011) conditions averaged over 2079-2099 and a CESM1 historical simulation averaged over 1979-2005. Thus, the perturbed sea surface temperatures and sea ice extent that forced the warmer future fvCAM5.1 simulations preserved the observed interannual variability over the nominal period 2079-2099 and will be referred to as "PlusRCP85." Volcanic aerosols and solar irradiance were preserved, but trace greenhouse gasses were altered to be consistent with the RCP8.5 protocols in the perturbed fvCAM5.1 simulation. The imposed global warming from CESM1 in these perturbations was equivalent to 3.8^{o}C with an equilibrium climate sensitivity of 4.1K (Meehl et al., 2013). This method of constructing perturbations to surface boundary conditions follows the methods of HAPPI ("Half a degree of Additional warming, Projections, and Prognosis and Impacts") experiments except (1) a single climate model was used instead of a multi-model ensemble, (2) a specific timeperiod and emissions scenario was chosen instead of a global warming level. Further details on ARTMIP experimental design are in Shields et al., 2018. AR tracking and analysis for fvCAM5.1 was conducted using 3-hourly IVT, IWV, and precipitation data. For quality control, the historical simulation is compared to MERRA-2 products (Gelaro et al., 2017) with fvCAM5.1 coarsened to MERRA-2 resolution (~50km) for direct comparisons. IWV and IVT were calculated from the 3-hourly zonal (U) and meridional (V) wind fields, and specific humidity (Q) and computed according to ARTMIP protocol (Shields et al., 2018). (Calculation details in supplemental material).

2.2. ARTMIP Experimental Design and Catalogues

ARTMIP is divided into two tiers that can be described by different levels of involvement. Tier 1, required for participation, serves as the baseline for subsequent experiments. Tier 2 is subdivided into different sensitivity experiments and is designed to test scientific questions. Examples of Tier2 studies include the reanalysis intercomparison across different global reanalysis products (Collow et al., 2022) and the CMIP5/6 climate change intercomparison

across different global, coupled climate models (O'Brien et al., 2022). ARDT developers participating in ARTMIP detect ARs using identical source data and create "catalogues" so that AR metrics can be directly compared. Catalogues are gridded, temporal datasets in which binary indicators of AR presence (AR tags) are defined at each grid point and each time slice. Details on participating algorithms are in Supplemental Table S1.

The design of the ARTMIP High-Resolution project required developers of ARDTs to produce catalogues for the historical period (1979 - 2005) and for end-of-the-century RCP 8.5 (2079 - 2099) to facilitate a comparison of ARs in two climates. Catalogues from two additional historical realizations (1995 - 2005) and one additional RCP 8.5 realization (2079 - 2084) were not required but generally contributed by participating groups. Unless otherwise noted, results incorporate all realizations. This experiment involved 14 catalogues from various ARDTs, all of which have contributed Tier 1 for a baseline comparison to earlier results in MERRA-2.

Tier 2 High Resolution (henceforth referred to as T2-HR) is different from Tier 2 CMIP5/6 (O'Brien et al., 2022), the companion climate change ARTMIP Tier 2 experiment, in several ways.

(1) T2-HR applies high horizontal resolution in a single model ensemble framework described above, while Tier 2 CMIP5/6 analyzed CMIP5 and 6 within a lower- resolution multi-model ensemble framework and a single simulation set (historical + future).
(2) T2-HR highlights bulk characteristics, such as spatial footprint and intensity, and AR impacts, such as precipitation in a warmer world, where Tier 2 CMIP5/6 primarily focused on analyzing climate trends demonstrating that ARDT uncertainty far outweighs model uncertainty.
(3) T2-HR describes regional detail for landfalling ARs, where CMIP5/6 generally focused on broad or global metrics.

Although global metrics are presented in this work, the primary purpose is to provide quality control between Tier 1 (MERRA-2 Reanalysis, herein referred to as T1-MERRA-2) and Tier 2 (T2-HR model simulations) as well as context for other ARTMIP experiments, both reanalysis

and CMIP5/6 experiments (Collow et al., 2022; O'Brien et al., 2022). Although O'Brien et al. (2022) classify ARDTs by threshold choices (absolute or relative; time-evolving or time-fixed), here we choose to classify by "restrictiveness" of thresholds to highlight two distinct climate response regimes, (1) one that allows for many ARs to be detected (less restrictive) and (2) another that imposes numerous restrictions and allows for fewer ARs to be detected (more restrictive). Dividing the ARDTs into these two regimes side-steps labeling ARDTs by parameter types and choices (Shields et al., 2018) and instead groups ARDTs by typical AR frequency (using Tier 1 as a baseline) and is easier to interpret for impacts. See Supplemental Table S2 for restrictiveness justification.

3 Global overview

To put the results of this paper into a global context, in this section we compare AR characteristics in the T2-HR dataset to those in the T1-MERRA-2 dataset for quality control and only the results for the global catalogues are shown in Figure 1 (see Table S1).

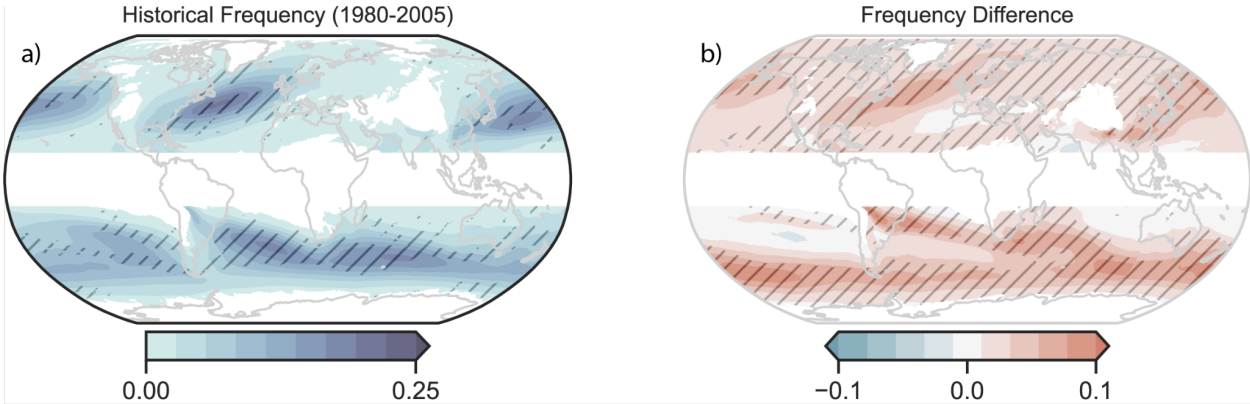

Figure 1. (a) Historical AR frequency (fraction of time across analysis period) where hatching shows at least half of ARDTs are within 10% of MERRA-2 values from Tier 1. (b) Relative difference between RCP85 and historical catalogues showing an overall increase in AR frequency over the mid-latitudes, where hatching shows 100% agreement in positive frequency between algorithms.

There is generally good agreement over main AR tracks and consistent with Tier2 CMIP5/6 (O'Brien et al., 2022), although the lack of hatching in the Pacific indicates historical simulations are over 10% of MERRA-2. Figure 1a explains the degree of agreement between T2-HR and T1-MERRA-2, and Figure 1b the fractional change in future AR frequency relative to the historical period (1979 - 2005). The average frequency is calculated for each algorithm for each dataset (e.g., historical, future and MERRA-2) then averaged across all ARDTs, respectively. There is a large range in the total number of events identified, but similarity of projected increases in frequency over the AR tracks with a slight expansion poleward. The most robust increases can be interpreted as locations where hatching exists in both panels, i.e., locations that most closely match MERRA-2 and full ARDT agreement. Further exploring global ARDTs, but directly comparing the spatial footprint and IVT intensity (Figure 2), a relationship between size and intensity emerges and illustrates methods with a high mean AR IVT correspond to smaller AR fractional areas, whereas methods with a large spatial footprint generally have lower mean IVT. This relationship holds across climate states. Intensity and size were calculated by focusing only on the AR objects for each algorithm. Fractional area is calculated as the fraction of AR objects over the globe, and IVT is calculated from the average (for each time slice) of the IVT maximum, minimum, and mean. Although restrictive ARDTs (Table S2) generally fall into the smaller footprint/higher IVT category, this is not always the case. For example, AR-CONNECT is a tracking methodology that relies on high thresholding to construct AR tracks but uses low thresholding requirements for growth and consequently AR size. High IVT values are common over the ocean but tend to decay at landfall, meaning that AR-CONNECT has lower coastal persistence (Figure S3) though over the oceans its characteristics resemble those from less restrictive methodologies. The difference in performance between coastlines and ocean locales in the AR-CONNECT demonstrates the importance of understanding the nuances of each ARDT, and the developmental intent of the algorithm, when applying to specific science problems. However, across all global ARDTs, methods with larger spatial footprint have a larger increase with climate change, although their mean IVT stays the same. Uniformly across ARDTs, the time-mean object-maximum IVT increases with global warming.

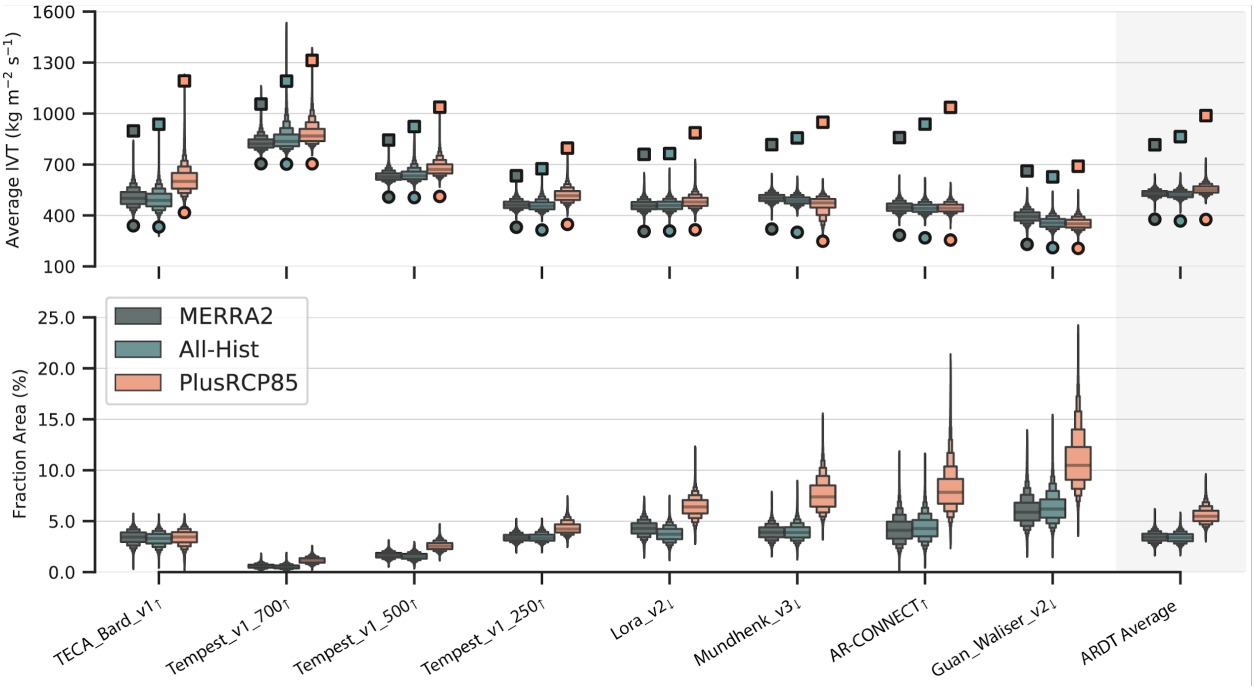

Figure 2. Boxenplot of (top row) object-mean AR IVT and (bottom row) fractional area for global ARDTs over the entire period (1979-2005, 2079-2099). The small boxes are mean object-maximum values over all time slices, small circles show mean object-minimum values over all time slices. Pink is the future climate, blue is the historical climate, and gray is MERRA-2. Global ARDTs are listed on the x-axis, and statistical boxes show the median (center line) with each outward level containing half the remaining data. Up (down) arrows next to ARDT names indicate restrictive (less restrictive) methods.

4 Regional Focus: Projected changes

One advantage of utilizing high resolution climate data is better representation of coastlines and geography. It is in this spirit that a regional analysis is performed for 5 subregions with frequent AR landfalls. Regional focus areas include (1) Western North America (32°N-52.5°N), (2) United Kingdom (49°N-60°N), (3) Iberian Peninsula (35°N-49°N), (4) South Africa (30°S-36°S), and (5) Southern South America (30°S-57°S). Subsetting ARDTs into two categories, i.e., those with restrictive (Figure 3 f-j) versus less restrictive requirements (a-e) and compiling frequency metrics across the historical and climate change simulations and MERRA-2 reanalysis, disagreement is evident in frequency across all months when quantifying the climate change

response. The range plotted in Figure 3 spans median to maximum frequency with climate change response in red bars and the historical in black bars. Less restrictive methods produce consistently higher occurrences in landfalling AR conditions across the entire period analyzed. Values have been normalized to percent (%) of time across each respective period. For some regions, such as landfalling ARs across Western North America and the Iberian Peninsula, there is essentially no difference between the historical spread versus the future climate spread for restrictive methods. For Western North American, this holds even if the region is subsetted between northern and southern latitudes (not shown). This result indicates that the climate change signal is sensitive to the detection method.

The MERRA-2 climatology is plotted for reference (gray bars) and illustrates that fvCAM5.1 is able to reproduce the seasonal cycle of ARs well. Magnitudes of frequency values are realistic, with only Western North America spring and summer seasons outside the MERRA-2 spread, where the model overproduces ARs. For northern hemisphere focus regions, both regional and global ARDTs are included and generally perform similarly. For the southern hemisphere regions, however, only global ARDTs are available and notably diverge in seasonality when comparing regional ARDTs from Tier 1 (Figure 3, Blamey et al., 2018, Viale et al., 2018). These Tier 1 southern hemisphere ARDTs are designed for their unique, respective regional AR characteristics. Comparing regional methods to global methods in these panels highlights discrepancies between ARDT climatologies for these locations. The largest discrepancy lies with South American ARs and can be tied to the latitudinal distribution (Figure S2). The regional ARDT (Viale et al., 2018) with relative IVT threshold (85th percentile) preferentially detects landfalling ARs between 50°S and 40ºS during wintertime, whereas the global methods detect ARs that dominate in the southernmost (south of 50°S) and subtropical bands. The higher AR frequency in summertime in South America by global methods compares more directly to UK AR climatology and storm track-driven AR occurrences. This suggests that global methods with fixed IVT threshold would produce an AR climatology in South America more weighted by the southernmost band with higher frequency of storm tracks. Although further investigations into the discrepancies between regional and global methodologies are subjects for future research, the uncertainty uncovered here supports past ARTMIP findings (Ralph et al., 2019, Rutz et al., 2019,

O’Brien et al., 2022, Collow et al. 2022, Shields et al. 2018) and highlights the importance of considering uncertainty arising from choice of ARDT.

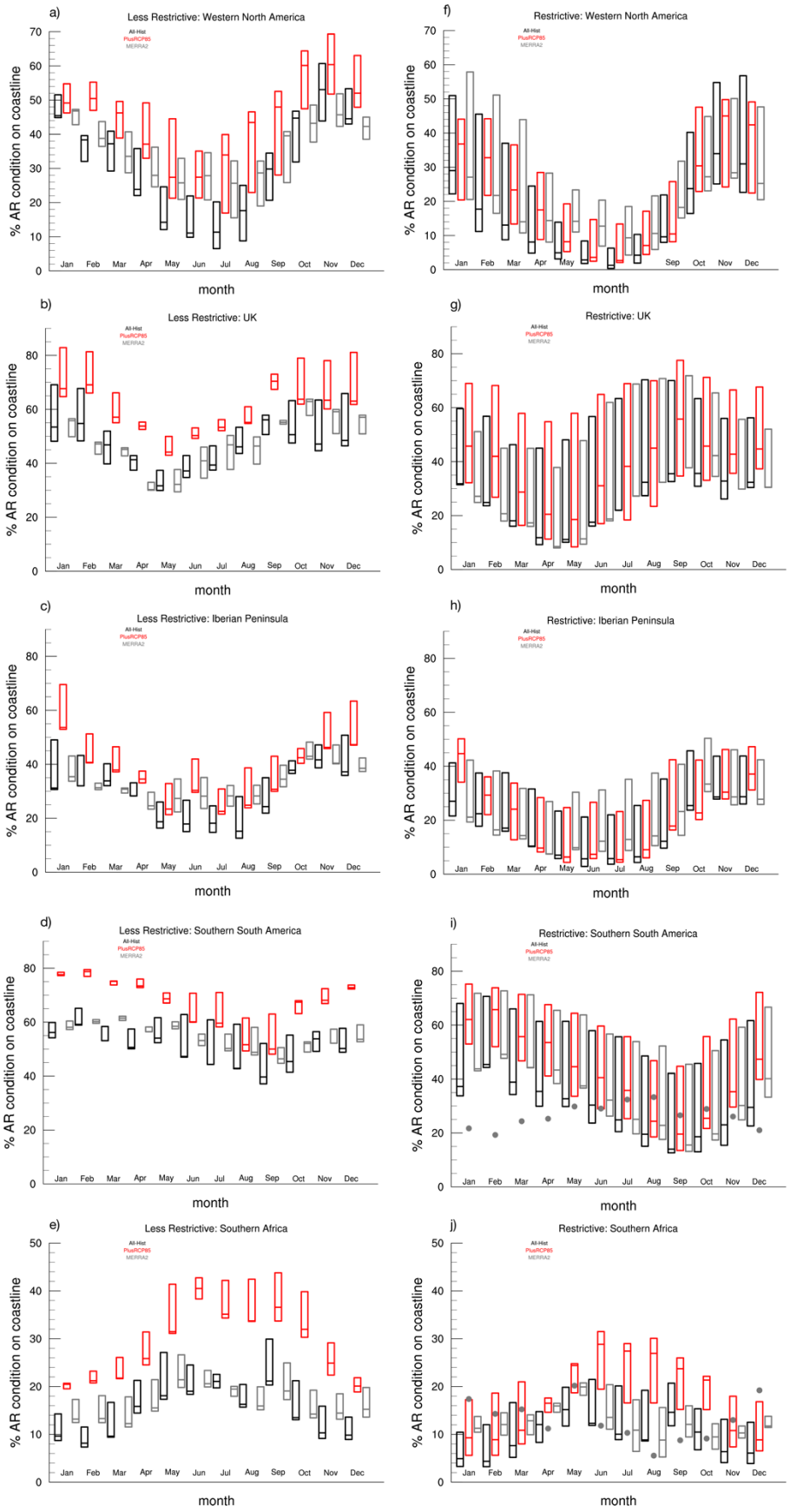
a)
Less Restrictive: Western North America
b)
Less Restrictive: UK
c)
Less Restrictive: Iberian Peninsula
d)
Less Restrictive: Southern South America
e)
Less Restrictive: Southern Africa
f)
Restrictive: Western North America
g)
Restrictive: UK
h)
Restrictive: Iberian Peninsula
i)
Restrictive: Southern South America
j)
Restrictive: Southern Africa
All-Hist
PlusRCP85
MERRA2
% AR condition on coastline
month
Jan
Feb
Mar
Apr
May
Jun
Jul
Aug
Sep
Oct
Nov
Dec

Figure 3. ARDT spread for landfalling AR occurrence climatology. The method with the median number of ARs is plotted as the lower bound, and the method with the most ARs, the upper bound. Tier 1 MERRA-2 (gray), Tier 2 high resolution "All-Hist" historical simulations (black), and Tier 2 high resolution "PlusRCP85" RCP8.5 (red). ARDTs are grouped by restrictiveness with less restrictive ARDTs (a-e) and more restrictive ARDTs (f-j). Regions include Western North America, United Kingdom, Iberian Peninsula, Southern South America, and Southern Africa (Coverage shown in S4). Gray dots in Southern Africa and Southern South America represent regional ARDTs from Tier 1 (Blamey et al., 2018, Viale et al., 2018). Although they did not participate in Tier2, they are shown to highlight discrepancies between regional and global ARDT climatologies. All other regions include both regional and global ARDTs that perform similarly with respect to seasonality. Because not all methods provide contributions for all ensemble members, frequency is given in % of time across analysis periods, scaling each ARDT contribution by number of years provided.

Regional evaluations of AR precipitation rate distributions and how they have changed between historical and global warming periods are shown in Figure 4. ARDT outputs are used to extract AR-linked precipitation from the climate model runs and are plotted based on intensity bins and each bin's fraction of total AR rainfall volume, as following techniques in Pendergrass and Hartman (2014a, b). For example, in Figure 4b, the mean ARDT results show that 1.5% of AR rainfall in the Northwest United States in the historical period comes at a rate of 200 mm/day or greater, while this jumps up to 4.3% in the RCP8.5 climate runs. Shaded envelopes show the spread of detected precipitation volume fractions per ARDT and the bold lines indicate mean values. Regional boxes (Figure S4) are defined using the same latitude limits as Figure 3. We choose to use a broad localized box centered around focus regions to maximize the character of the impact from precipitation in these regions that incorporate land points, coastlines, and regional ocean influences. A general pattern emerges from all regions: a decrease from baseline in rainfall volume fraction at the lower end of the intensity spectrum (roughly the 3-30 mm/day range) and an increase in the higher 50-200+ mm/day range. In all regions, the differences between periods at these intensity bins cannot overcome the range of ARDT spread, indicating that an intensification signal is sensitive to ARDT selection, illustrating the necessity of considering an ensemble of techniques to investigate AR science questions as recommended in

O'Brien et al. (2021). The most noticeable difference in spreads occurs in the British Islands (UK), where a particularly large signal is evident in the 50-200 mm/day range, showcasing a large change in precipitation volumes between periods. This result falls in line with expected intensification of AR precipitation at the extreme end of the spectrum (Wuebbles et al. 2017; IPCC WG1 Chapter 8 (Douville et al. 2021), Chapter 11 (Seneviratne et al., 2021)) and is consistent with other AR studies that show a shift towards more extreme precipitation (Shields and Kiehl, 2016a, Polade et al., 2017, Gershunov et al., 2019). It is also consistent with global warming studies that demonstrate the increase in heavy precipitation is tied to both the expansion of the subtropics, thus pushing mid-latitude cyclones poleward, and wetter ARs due to thermodynamics (Gerhunov et al., 2019, Shields and Kiehl, 2016b, Baek and Lora, 2021). Other noteworthy results of interest are the relatively large change in upper tail (200+ mm/day) rainfall in South Africa between periods and the relatively low change between periods in South America. Because uncertainty across ARDTs generally increases as the AR reaches further inland (Collow et al., 2022), the AR-precipitation spread impacting land points only was also considered and found to be similar, although the ARDT spread is wider (Figure S5).

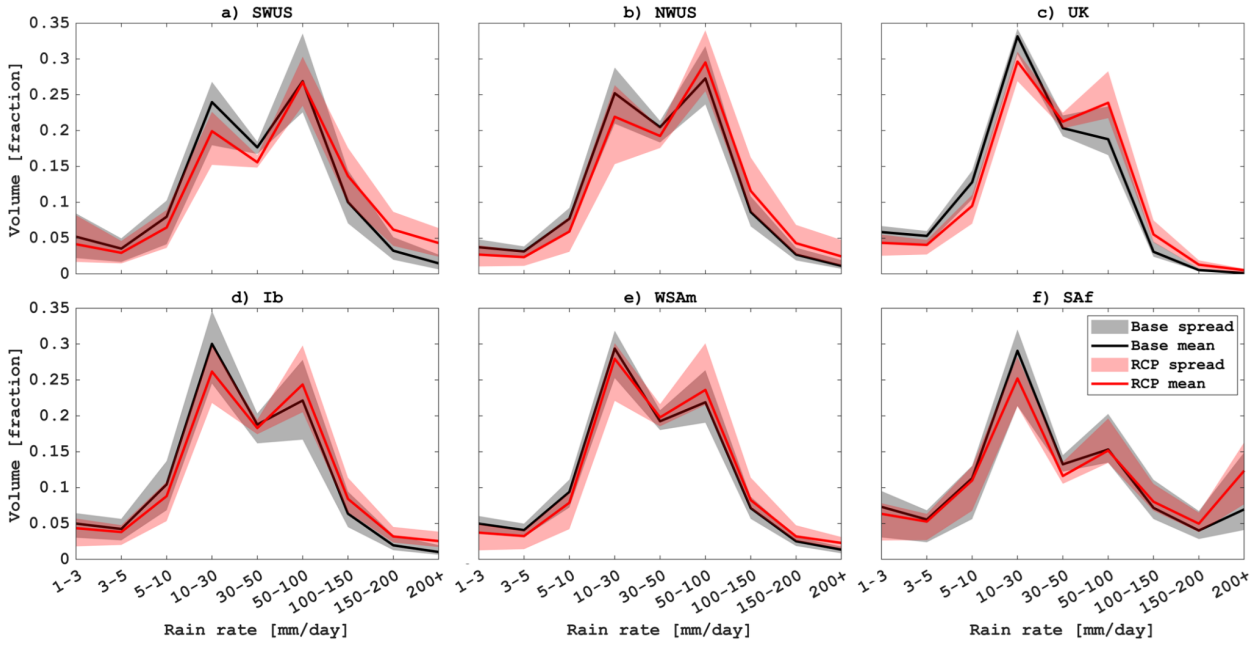

Figure 4. Distribution of rainfall rates produced by ARs calculated as its fraction of total AR precipitation volume during the baseline (All-Hist) period shown in black and RCP8.5 period

shown in red, distributed by rainfall rate. The shaded envelopes show distribution of all ARDT methodologies, all T2-HR simulations, encompassing the mean values shown by thick lines. Each subfigure indicates distributions from different regions (Figure S4) of frequent AR landfall: a) Southwestern US, b) Northwestern US, c) the British Isles, d) Iberia, e) Southwestern South America, and f) Southern Africa.

5 Discussion and Summary

High-resolution historical and future climate simulations are used to evaluate ARDTs for both global and regional domains. High horizontal model resolution is applied to better represent bulk AR characteristics, regional geography to landfalling locations, and more accurate precipitation and extremes. Historical simulations produced by fvCAM5.1 produce realistic AR metrics for frequency, intensity, global distribution, and seasonality. The methods also broadly support the notion that AR frequency and intensity will increase in a warmer, future climate, although regional differences exist, especially regarding the magnitude of the increases and their spatial distribution. The current literature shows the thermodynamic response dominates AR changes (e.g. Michaelis et al., 2022, Payne et al., 2020, Gershunov et al., 2019, Gao et al. 2015, Lavers et al., 2013, Baek and Lora, 2021), but the degree to which the ARs respond to climate change is highly uncertain (O'Brien et al. 2022). ARTMIP Tier 2 CMIP5/6 shows that the uncertainty across ARDTs in the AR frequency trends far surpasses the uncertainty across climate models. Here, HR-T2 analysis shows that the restrictiveness of the algorithmic parameters largely explains the scale of the response, despite agreement in bulk characteristics. Across global algorithms, IVT intensity and spatial footprint are inversely correlated, such that methods with higher IVT intensity tend to have a smaller spatial footprint. With a less restrictive algorithm, more ARs are detected but with a lower average AR IVT.

Seasonally, regional methods and global methods also tend to behave similarly, but only in the northern hemisphere. For example, global ARDTs applied to South America have a distinctly different climatology compared to Tier 1 regional ARDTs which can be tied to the dominant type of ARs detected. Applying a South American-specific ARDT (Viale et al. 2018), the

dominant ARs lie in the storm track south of 40°S whereas the global ARs tend to detect more ARs in the subtropics. Despite these regional nuances, even from a seasonal viewpoint, restrictive algorithms detect far fewer ARs than less restrictive ones and display a far weaker climate change signal consistent across all focus regions. Simply, the choice of ARDT can determine whether a climate change signal is present at all.

Regarding precipitation attributable to ARs compared across ARDTs, like bulk characteristics, precipitation distributions align well with each other across regional focus areas; however, precipitation amounts span a wide envelope of possibilities. Under the RCP8.5 scenario and consistent with current literature, precipitation intensity generally increases for more extreme precipitation rates, and decreases for light rates, yet the spread of values across ARDTs for RCP8.5 conditions falls within the spread for the historical, thus adding to previous ARTMIP conclusions that uncertainty due to ARDT overwhelms metrics dependent on AR frequency numbers. Ultimately, relying on one ARDT, or ARDTs too similar to each other without understanding algorithmic sensitivities, does a disservice to quantifying AR impacts. Given that precipitation generated or transported by ARs is used to quantify water availability for many local communities, changes to AR precipitation, and the uncertainty associated with any AR metric, is highly relevant for water resource planning now (Michaelis et al., 2022) and in the coming decades.

Tier2-HR illustrates the necessity of understanding ARDTs sensitivities when choosing methodologies suitable for the science question posed. If possible, a selection of ARDTs should be applied to climate change AR analysis that applies both restrictive and nonrestrictive groups. Type of AR and/or regional focus area matter. Restrictive ARDTs applied to Western North America and the Iberian Peninsula produce a climatology that is essentially unchanged for a future climate compared to less restrictive algorithms for the same area. Minimally, for climate change AR analysis, an evaluation of the ARDT's restrictiveness, and AR metrics compared to other published ARDTs, should be standard procedure to alert readers to both context and associated uncertainties.

6 References

Albano, C. M., Dettinger, M. D., & Harpold, A. A. (2020). Patterns and drivers of atmospheric river precipitation and hydrologic impacts across the western United States. Journal of Hydrometeorology, 21(1), 143-159.

American Meteorological Society: Atmospheric River, Glossary of Meteorology, available at: http://glossary.ametsoc.org/wiki/ atmosphericriver (last access: 24 October 2022), 2017.

Baek, S.H., Lora, J.M. Counterbalancing influences of aerosols and greenhouse gases on atmospheric rivers. Nat. Clim. Chang. 11, 958–965 (2021). https://doi.org/10.1038/s41558-021-01166-8

Blamey, R. C., Ramos, A. M., Trigo, R. M., Tomé, R., & Reason, C. J. C. (2018). The Influence of Atmospheric Rivers over the South Atlantic on Winter Rainfall in South Africa, Journal of Hydrometeorology, 19(1), 127-142.

Collow, A.B., Shields, C.A., Guan, B., Kim, S., Lora, J.M., McClenny, E.E., Nardi, K., Payne, A., Reid, K., Shearer, E. J. , Tome, R., Wille, J.D., Ramos, A.M., Gorodetskaya, I.V., Leung, L.R., O'Brien, T.A., Ralph, F.M., Rutz, J. Ullirich, P.A., Wehner, M., (2022) An Overview of ARTMIP's Tier 2 Reanalysis Intercomparison: Uncertainty in the Detection of Atmospheric Rivers and their Associated Precipitation, Journal of Geophysical Research, Atmospheres, 127, https://agupubs.onlinelibrary.wiley.com/doi/10.1029/2021JD036155.

Corringham, T.W., McCarthy, J., Shulgina, T. et al. Climate change contributions to future atmospheric river flood damages in the western United States. Sci Rep 12, 13747 (2022). https://doi.org/10.1038/s41598-022-15474-2

Demory, M.-E., Berthou, S., Fernández, J., Sørland, S. L., Brogli, R., Roberts, M. J., Beyerle, U., Seddon, J., Haarsma, R., Schär, C., Buonomo, E., Christensen, O. B., Ciarlo`, J. M., Fealy, R., Nikulin, G., Peano, D., Putrasahan, D., Roberts, C. D., Senan, R., Steger, C., Teichmann, C., and Vautard, R.: European daily precipitation according to EURO-CORDEX regional climate

models (RCMs) and high-resolution global climate models (GCMs) from the High-Resolution Model Intercomparison Project (HighResMIP), Geosci. Model Dev., 13, 5485–5506, https://doi.org/10.5194/gmd-13-5485-2020, 2020.

Douville, H., K. Raghavan, J. Renwick, R.P. Allan, P.A. Arias, M. Barlow, R. Cerezo-Mota, A. Cherchi, T.Y. Gan, J. Gergis, D. Jiang, A. Khan, W. Pokam Mba, D. Rosenfeld, J. Tierney, and O. Zolina, 2021: Water Cycle Changes. In Climate Change 2021: The Physical Science Basis. Contribution of Working Group I to the Sixth Assessment Report of the Intergovernmental Panel on Climate Change [Masson-Delmotte, V., P. Zhai, A. Pirani, S.L. Connors, C. Péan, S. Berger, N. Caud, Y. Chen, L. Goldfarb, M.I. Gomis, M. Huang, K. Leitzell, E. Lonnoy, J.B.R. Matthews, T.K. Maycock, T. Waterfield, O. Yelekçi, R. Yu, and B. Zhou (eds.)]. Cambridge University Press, Cambridge, United Kingdom and New York, NY, USA, pp. 1055–1210, doi:10.1017/9781009157896.010.

Espinoza, V., Waliser, D. E., Guan, B., Lavers, D. A., & Ralph, F. M. (2018). Global analysis of climate change projection effects on atmospheric rivers. Geophysical Research Letters, 45(9), 4299-4308.

Gao, Y., J. Lu, L. R. Leung, Q. Yang, S. Hagos, and Y. Qian (2015), Dynamical and thermodynamical modulations on future changes of landfalling atmospheric rivers over western North America, Geophys. Res. Lett., 42, 7179–7186, doi:10.1002/2015GL065435.

Gershunov, A., T.M. Shulgina, R.E.S. Clemesha, K. Guirguis, D.W. Pierce, M.D. Dettinger, D.A. Lavers, D.R. Cayan, S.D. Polade, J. Kalansky and F.M. Ralph, 2019: Precipitation regime change in Western North America: The role of Atmospheric Rivers. Nature Scientific Reports, 9:9944, DOI: 10.1038/s41598-019-46169-w. https://rdcu.be/bJPK0

Griffith, HV, Wade, AJ, Lavers, DA, Watts, G. Atmospheric river orientation determines flood occurrence. Hydrological Processes. 2020; 34: 4547– 4555. https://doi.org/10.1002/hyp.13905

Guan, B., & Waliser, D. E. (2017). Atmospheric rivers in 20 year weather and climate simulations: A multimodel, global evaluation. Journal of Geophysical Research: Atmospheres, 122(11), 5556–5581. https://doi.org/10.1002/2016JD026174

Hurrell, J. W., Holland, M. M., Gent, P. R., Ghan, S., Kay, J. E., Kushner, P. J., et al. (2013). The Community Earth System Model: A framework for collaborative research. Bulletin of the American Meteorological Society, 94(9), 1339–1360. https://doi.org/10.1175/BAMS-D- 12-00121.1

Lavers, D. A., R. P. Allan, G. Villarini, B. Lloyd-Hughes, D. J. Brayshaw, and A. J. Wade (2013), Future changes in atmospheric rivers and their implications for winter flooding in Britain, Environ. Res. Lett., 8, 034,010, doi:10.1088/1748-9326/8/3/034010.

Lora, J. M., Shields, C. A., & Rutz, J. J., (2020), Consensus and disagreement in atmospheric river detection: ARTMIP global catalogues. Geophysical Research Letters, 47, e2020GL089302,https://doi.org/10.1029/2020GL089302.

Michaelis, A. C., Gershunov, A., Weyant, A., Fish, M. A., Shulgina, T., & Ralph, F. M. (2022). Atmospheric river precipitation enhanced by climate change: A case study of the storm that contributed to California's Oroville Dam crisis. Earth's Future, 10, e2021EF002537. https://doi.org/10.1029/2021EF002537.

Meehl, Gerald A., Warren M. Washington, Julie M. Arblaster, Aixue Hu, Haiyan Teng, Jennifer E. Kay, Andrew Gettelman, David M. Lawrence, Benjamin M. Sanderson, and Warren G. Strand. "Climate Change Projections in CESM1(CAM5) Compared to CCSM4", Journal of Climate 26, 17 (2013): 6287-6308, https://doi.org/10.1175/JCLI-D-12-00572.1

O'Brien, T. A., Wehner, M. F., Payne, A. E., Shields, C. A., Rutz, J. J., Leung, L.-R., et al. (2022). Increases in future AR count and size: Overview of the ARTMIP Tier 2 CMIP5/6 experiment. *Journal of Geophysical Research: Atmospheres*, 127, e2021JD036013. https://doi.org/10.1029/2021JD036013

O'Brien, T. A., and Coauthors, 2020: Detection Uncertainty Matters for Understanding Atmospheric Rivers. Bull. Amer. Meteor. Soc., 101, E790–E796, Bull. Amer. Meteor. Soc. , https://doi.org/10.1175/BAMS-D-19-0348.1

Paltan, H., Waliser, D., Lim, W. H., Guan, B., Yamazaki, D., Pant, R., & Dadson, S. (2017). Global floods and water availability driven by atmospheric rivers. Geophysical Research Letters, 44, 10,387– 10,395. https://doi.org/10.1002/2017GL074882

Pan, M., & Lu, M. (2020). East Asia Atmospheric River catalog: Annual cycle, transition mechanism, and precipitation. Geophysical Research Letters, 47, e2020GL089477. https://doi.org/10.1029/2020GL089477

Payne, A.E., Demory, M., Leung, L.R., Ramos, A., Shields C.A., Rutz, J. J., Siler, N., Villarini, G., Hall, A., Ralph, F. M., Responses and impacts of atmospheric rivers to climate change. Nat Rev Earth Environ 1, 143–157, https://doi.org/10.1038/s43017-020-0030-5 , 2020.

Pendergrass, A. G., & Hartmann, D. L. (2014a). Changes in the Distribution of Rain Frequency and Intensity in Response to Global Warming*. Journal of Climate, 27(22), 8372–8383. https://doi.org/10.1175/JCLI-D-14-00183.1

Pendergrass, A. G., & Hartmann, D. L. (2014b). Two Modes of Change of the Distribution of Rain*. Journal of Climate, 27(22), 8357–8371. https://doi.org/10.1175/JCLI-D-14-00182.1

Polade, S.D., A. Gershunov, D.R. Cayan, M.D. Dettinger and D.W. Pierce, 2017: Precipitation in a warming world: Assessing projected hydro-climate of California and other Mediterranean climate regions. Nature Scientific Reports, 7: 10783, DOI:10.1038/s41598-017-11285-y.

Ralph, F. M., Wilson, A. M., Shulgina, T., Kawzenuk, B., Sellars, S., Rutz, J. J., … Wick, G. A. (2019). ARTMIP-early start comparison of atmospheric river detection tools: how many

atmospheric rivers hit northern California's Russian River watershed?. Climate Dynamics, 52(7-8), 4973-4994. doi: 10.1007/s00382-018-4427-5

Ralph, F. M., Dettinger, M. D., Cairns, M. M., Galarneau, T. J., & Eylander, J. (2018). Defining "Atmospheric River": How the Glossary of Meteorology Helped Resolve a Debate, *Bulletin of the American Meteorological Society*, 99(4), 837-839.

Ralph, F. M., Dettinger, M., Lavers, D., Gorodetskaya, I. V., Martin, A., Viale, M., ... & Cordeira, J. (2017). Atmospheric rivers emerge as a global science and applications focus. Bulletin of the American Meteorological Society, 98(9), 1969-1973.

Ramos, Alexandre M., Ricardo M. Trigo, Margarida L. R. Liberato, and Ricardo Tomé. "Daily Precipitation Extreme Events in the Iberian Peninsula and Its Association with Atmospheric Rivers". Journal of Hydrometeorology 16.2 (2015): 579-597. <https://doi.org/10.1175/JHM-D-14-0103.1>

Reid, K. J., King, A. D., Lane, T. P., & Hudson, D. (2022). Tropical, Subtropical, and Extratropical Atmospheric Rivers in the Australian Region. Journal of Climate, 35(9), 2697-2708.

Rhoades, A. M., Risser, M. D., Stone, D. A., Wehner, M. F., & Jones, A. D. (2021). Implications of warming on western United States landfalling atmospheric rivers and their flood damages. Weather and Climate Extremes, 32, 100326.

Rutz, J.J, Shields, C.A., Lora, J.M, Payne, A.E., Guan, B., Ullrich, P., O'Brien, T., Leung, L.-Y., Ralph, F.M., Wehner, M., Brands, S., Collow, A., Goldenson, N., Gorodetskaya, I., Griffith, H., Hagos, S., Kashinath, K., Kawzenuk, B., Krishnan, H., Kurlin, V., Lavers, D., Magnusdottir, G., Mahoney, K., McClenny, E., Muszynski, G., Nguyen, P.D., Prabhat, Qian, Y., Ramos, A.M., Sarangi, C., Sellars, S., Shulgina, T., Tome, R., Waliser, D., Walton, D., Wick, G., Wilson, A., Viale, M.: The Atmospheric River Tracking Method Intercomparison Project (ARTMIP):

Quantifying Uncertainties in Atmospheric River Climatology, Journal of Geophysical Research-Atmospheres , https://doi.org/10.1029/2019JD030936, 2019.

Sadeghi, M., Shearer, E. J., Mosaffa, H., Gorooh, V. A., Naeini, M. R., Hayatbini, N., ... & Sorooshian, S. (2021). Application of remote sensing precipitation data and the CONNECT algorithm to investigate spatiotemporal variations of heavy precipitation: Case study of major floods across Iran (Spring 2019). Journal of Hydrology, 600, 126569.

Schick, L.J. et al. (2020). Applications of Knowledge and Predictions of Atmospheric Rivers. In: Ralph, F., Dettinger, M., Rutz, J., Waliser, D. (eds) Atmospheric Rivers. Springer, Cham. https://doi.org/10.1007/978-3-030-28906-5_7.

Seneviratne, S.I., X. Zhang, M. Adnan, W. Badi, C. Dereczynski, A. Di Luca, S. Ghosh, I. Iskandar, J. Kossin, S. Lewis, F. Otto, I. Pinto, M. Satoh, S.M. Vicente-Serrano, M. Wehner, and B. Zhou, 2021: Weather and Climate Extreme Events in a Changing Climate. In Climate Change 2021: The Physical Science Basis. Contribution of Working Group I to the Sixth Assessment Report of the Intergovernmental Panel on Climate Change [Masson-Delmotte, V., P. Zhai, A. Pirani, S.L. Connors, C. Péan, S. Berger, N. Caud, Y. Chen, L. Goldfarb, M.I. Gomis, M. Huang, K. Leitzell, E. Lonnoy, J.B.R. Matthews, T.K. Maycock, T. Waterfield, O. Yelekçi, R. Yu, and B. Zhou (eds.)]. Cambridge University Press, Cambridge, United Kingdom and New York, NY, USA, pp. 1513–1766, doi:10.1017/9781009157896.013.

Shields, C. A., Wille, J. D., Marquardt Collow, A. B., Maclennan, M., & Gorodetskaya, I. V. (2022). Evaluating uncertainty and modes of variability for Antarctic atmospheric rivers. Geophysical Research Letters, 49, e2022GL099577. https://doi.org/10.1029/2022GL099577

Shields, C.A., J.J. Rutz, L.R. Leung, F.M. Ralph, M. Wehner, T. O'Brien, and R. Pierce, 0: Defining Uncertainties Through Comparison of Atmospheric River Tracking Methods. Bull. Amer. Meteor. Soc., 0, https://doi.org/10.1175/BAMS-D-18-0200.1 , 2019.

Shields, C. A., Rutz, J. J., Leung, L.-Y., Ralph, F. M., Wehner, M., Kawzenuk, B., Lora, J. M., McClenny, E., Osborne, T., Payne, A. E., Ullrich, P., Gershunov, A., Goldenson, N., Guan, B., Qian, Y., Ramos, A. M., Sarangi, C., Sellars, S., Gorodetskaya, I., Kashinath, K., Kurlin, V., Mahoney, K., Muszynski, G., Pierce, R., Subramanian, A. C., Tome, R., Waliser, D., Walton, D., Wick, G., Wilson, A., Lavers, D., Prabhat, Collow, A., Krishnan, H., Magnusdottir, G., and Nguyen, P.: Atmospheric River Tracking Method Intercomparison Project (ARTMIP): project goals and experimental design, Geosci. Model Dev., 11, 2455-2474, https://doi.org/10.5194/gmd-11-2455-2018, 2018.

Shields, C. A., and J. T. Kiehl (2016a),Simulating the Pineapple Express in the half degree Community Climate System Model, CCSM4, Geophys. Res. Lett., 43, doi:10.1002/2016GL069476.

Shields, C. A., & Kiehl, J. T. (2016b). Atmospheric river landfall-latitude changes in future climate simulations. Geophysical Research Letters, 43, 8775-8782. doi:10.1002/2016GL070470

Shields, C. A., Kiehl, J. T. and Meehl, G. A. (2016), Future changes in regional precipitation simulated by a half degree coupled climate model: Sensitivity to horizontal resolution. J. Adv. Model. Earth Syst.. , doi:10.1002/2015MS000584.

Sousa, P. M., Blamey, R. C., Reason, C. J., Ramos, A. M., & Trigo, R. M. (2018). The 'Day Zero'Cape Town drought and the poleward migration of moisture corridors. Environmental Research Letters, 13(12), 124025.

van Vuuren, D.P., Edmonds, J., Kainuma, M. *et al.* The representative concentration pathways: an overview. *Climatic Change* 109, 5 (2011). https://doi.org/10.1007/s10584-011-0148-z.

Viale, M., Valenzuela, R., Garreaud, R. D., & Ralph, F. M. (2018). Impacts of Atmospheric Rivers on Precipitation in Southern South America, Journal of Hydrometeorology, 19(10), 1671-1687.

Wehner, M.,F., Reed, K., Li, F., Prabhat, Bacmeister, J.,Chen, C-T., Paciorek, C., Gleckler, P., Sperber, K.,Collins, W.D., Gettelman, A., Jablonowski, C.(2014) The effect of horizontal resolution on simulation quality in the Community Atmospheric Model, CAM5.1. *Journal of Modeling the Earth System* 06, 980-997. doi:10.1002/2013MS000276

Wuebbles, D.J., D.R. Easterling, K. Hayhoe, T. Knutson, R.E. Kopp, J.P. Kossin, K.E. Kunkel, A.N. LeGrande, C. Mears, W.V. Sweet, P.C. Taylor, R.S. Vose, and M.F. Wehner, 2017: Our globally changing climate. In Climate Science Special Report: Fourth National Climate Assessment, Volume I. D.J. Wuebbles, D.W. Fahey, K.A. Hibbard, D.J. Dokken, B.C. Stewart, and T.K. Maycock, Eds. U.S. Global Change Research Program, pp. 35-72, doi:10.7930/J08S4N35.

Zhu, Y., and R. E. Newell (1998), A proposed algorithm for moisture fluxes from atmospheric rivers, Mon. Weather Rev., 126(3), 725–735, doi:10.1175/1520-0493(1998)126<0725:APAFMF>2.0.CO;2.

7 Acknowledgements

We have many thanks to give. ARTMIP is a grass-roots community effort and includes a large collection of international researchers from universities, laboratories, and agencies. It has received support from the US Department of Energy Office (DOE) of Science Biological and Environmental Research (BER) as part of the Regional and Global Climate Modeling program (RGMA), and the Center for Western Weather and Water Extremes (CW3E) at Scripps Institute for Oceanography at the University of California. Shields, O'Brien, Wehner, Lueng, Qian, Sarangi, Zarzycki acknowledge DOE (BER) RGMA, a component of the Earth and Environmental System Modeling Program with Award Numbers DE-SC0022070 (Shields), DE-AC02-05CH11231 (O'Brien, Wehner, McClenny), DE-AC05-76RL01830 (Leung, Qian, Sarangi) through the Water Cycle and Climate Extremes Modeling (WACCEM) scientific focus area, DE-SC0016605 (Ullrich, McClenny, C, Zarzycki) through "A framework for improving analysis and modeling of Earth system and intersectoral dynamics at regional scales". Additionally, support has been given from the National Science Foundation (NSF) IA 1947282 and National Center for Atmospheric Research (NCAR) under Cooperative Agreement No. 1852977 (Shields); the Environmental Resilience Institute, funded by Indiana University's

Prepared for Environmental Change Grand Challenge initiative (O'Brien); Lilly Endowment Inc., through its support for the Indiana University Pervasive Technology Institute (O'Brien); Pacific Northwest National Laboratory operated for DOE by the Battelle Memorial Institute under contract DE-AC05-76RL01830 (Leung, Qian, Sarangi); the National Institute of Food and Agriculture, U.S. Department of Agriculture, hatch project under California Agricultural Experiment Station project accession nos. 1010971 and 1016611 (McClenny); Ridge to Reef NSF Research Traineeship (#DGE-1735040), California Energy Commission (#300-15-005), CW3E at the Scripps Institution of Oceanography via AR Program Phase II (#4600013361) sponsored by CA-DWR (Shearer); NASA's Earth Science Research Program (Collow); Climate Process Team (CPT) under Grant AGS-1916689 from the NSF and Grant NA19OAR4310363 from the National Oceanic and Atmospheric Administration (NOAA) (Nardi); the Hong Kong Research Grants Council funded projects #16200920 and collaborative research fund # C6032-21G, (Dong, Lu, Pan); New Faculty Initiation Grant project number CE/20-21/065/NFIG/008961 from IIT Madras, India (Sarangi); NASA grants 80NSSC20K1344 and 80NSSC21K1007, and the California Department of Water Resources (Guan); the Helmholtz "Changing Earth" program (Ramos); the Portuguese Fundação para a Ciência e a Tecnologia (FCT) I.P./MCTES through national funds (PIDDAC) – UIDB/50019/2020 (Tomé); FONCYT PICT-2020-11722 (Viale); SCENARIO-CASE studentship, funded jointly by the UK Natural Environment Research Council and the UK Environment Agency under award code NE/P010040/1 (Griffith). Finally, we thank ARTMIP contributor Naomi Goldenson for providing ARDT catalogues to this project.

Open Research

ARTMIP catalogues and source data (MERRA-2 and CAM5 data) can be found on the Climate Data Gateway website, https://www.earthsystemgrid.org/dataset/ucar.cgd.artmip.html.